

HIGH MASS SINGLE DIFFRACTION EXCITATION IN $dp \rightarrow dX$ AT $s = 2800 \text{ GeV}^2$

J.C.M. Armitage, P. Benz, G.J. Bobbink, F.C. Ern , P. Kooijman,
F.K. Loebinger, A.A. Macbeth, H.E. Montgomery, P.G. Murphy,
J.J.M. Poorthuis, A. Rudge, J.C. Sens, D. Stork, J. Timmer

CERN, Geneva, Switzerland

Daresbury Laboratory, U.K.

Foundation for Fundamental Research on Matter, (F.O.M.), The Netherlands

University of Manchester, U.K.

University of Utrecht, The Netherlands

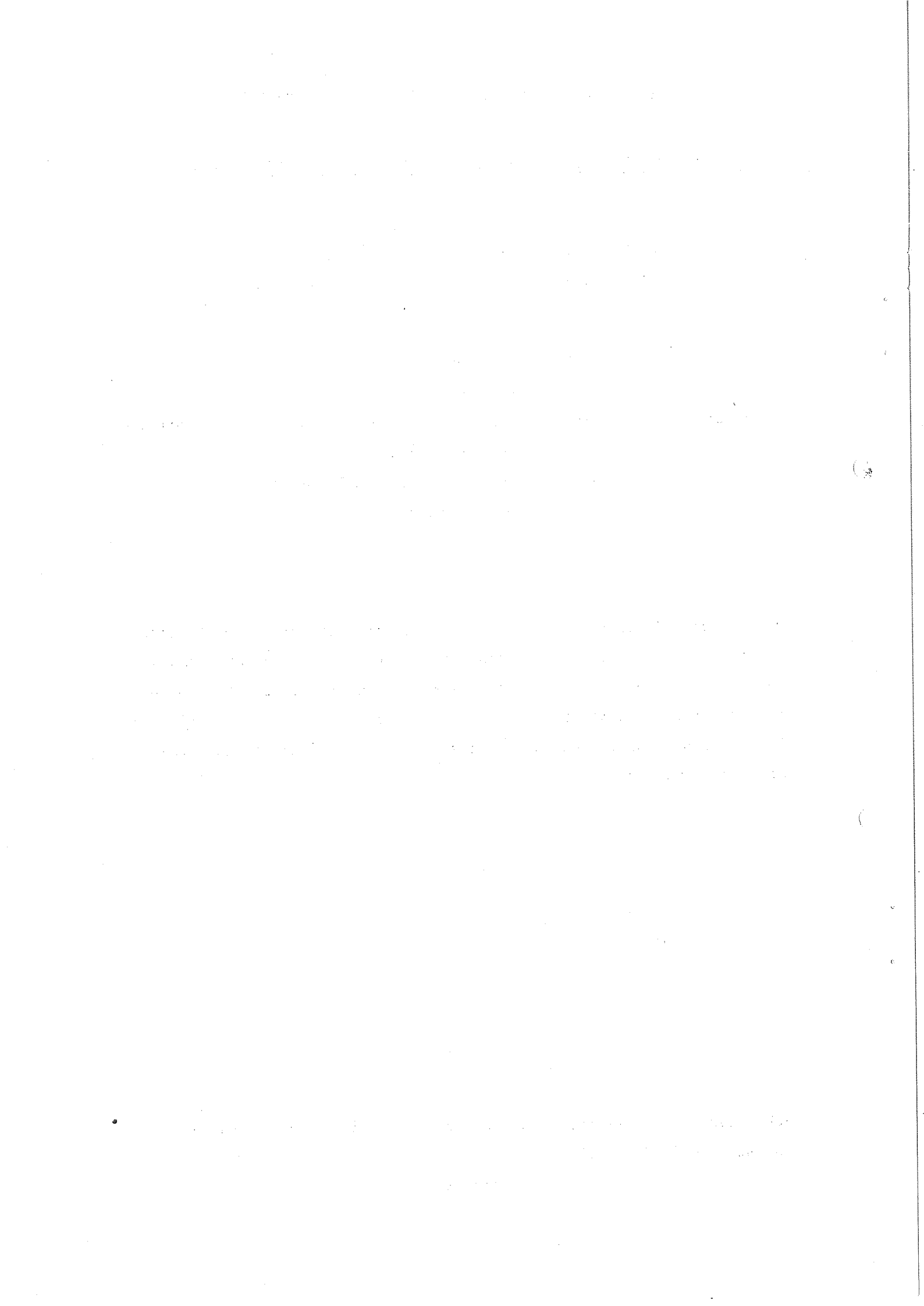
(CHM Collaboration)

Abstract

Data on $dp \rightarrow dX$ at $s = 2800 \text{ GeV}^2$ are presented. The measurements were performed with a single arm magnetic spectrometer at momentum transfers t between $- .20$ and $- .35 (\text{GeV}/c)^2$. The data are compared with proton spectra in $pp \rightarrow pX$ at the same energy for the kinematic region $M_x^2 < 360 \text{ GeV}$ where M_x^2 denotes the mass of the system X recoiling against the measured particle.

Submitted to the International Conference on High Energy Physics,
Tbilisi 15 - 21 July 1976.

May 1976



Data on the inclusive reaction $dp \rightarrow dX$ at $\sqrt{s} = 52$ GeV are presented. The deuteron is detected in the kinematic region $.85 < x < 1.0$ and $-.4 < t < -.2$ $(\text{GeV}/c)^2$ where x is the Feynman variable ($x = \frac{2p_L}{\sqrt{s}}$) and t is the square of the four momentum transfer between the initial and final state deuterons.

The data were taken with a magnetic spectrometer consisting of one magnet, 14 planes of magnetostrictive spark chambers and 4 trigger counters. The spectrometer was placed downstream of the intersection region, under the circulating deuteron beam in Intersection 2 of the CERN ISR. The mean angle which the spectrometer accepted could be varied from 15 to 90 mrad with respect to the primary beam (Fig. 1). The momentum resolution of the spectrometer was $\frac{\Delta p}{p} \sim 3\%$ (FWHM). For the data presented here the spectrometer was set to accept particles produced between 15 and 25 mrad and with a momentum greater than ~ 10 GeV/c. Furthermore the intersection region was surrounded by hodoscopes consisting in total of 186 scintillation counters covering 95% of the full solid angle, one of which was positioned directly opposite the spectrometer and had a fine angular binning ($\Delta\theta \sim 12$ mrad). A second spectrometer (described in ref. 5), situated above ring 1, was briefly used for a calibration run, described below. The relevant part of this spectrometer was an ethylene Cerenkov which could be pressurised to 30 atmospheres, and used for deuteron-proton separation.

The main aim of this experiment was to obtain a more accurate measurement of the Pomeron (diffractive) contribution to high- x inelastic scattering at ISR energies. One well known theoretical model used in the analysis of high x scattering is the Triple-Regge model. This relates the contribution of the exchange of a given Reggeon R_i in the quasi-two-body process

$$ab \rightarrow cX$$

(see Fig. 2a)), to a Triple-Reggeon coupling diagram (see Fig. 2b)) via the generalised optical theorem¹). If the $ab \rightarrow cX$ is diffractive i.e. a and c have identical quantum numbers then R_i can be equated to the

Pomeron. Many measurements of the process $pp \rightarrow pX$ have been performed and attempts to fit these have been made using the Triple-Regge picture. Since the proton may also be produced non-diffractively a complete fit must take into account all possible (R_i, R_j, R_k) -couplings. A typical fit is shown in Fig. 3 from T. Inami and R.G. Roberts²). One sees that the most significant non-PPP background is a term classified as ' π exchange'. If this picture holds then in dp scattering the ' π exchange' term should vanish because of Isospin conservation. Thus in dp scattering the non-PPP background should be smaller and should yield a cleaner diffractive signal.

Fig. 4 shows the observed momentum spectrum integrated over the angular range of the spectrometer and not corrected for its momentum acceptance. One sees two clear peaks one centered at the momentum of the primary beam (coherently scattered deuterons), the second centered around half the primary beam momentum. The second peak consists of protons from scattering processes in which the deuteron has broken up. The detected proton is either a spectator from a proton-neutron scattering event or a product of a proton-proton scattering event. The two processes can be written as

$$pn(p_s) \rightarrow X(p_{s,d})$$

$$pp(n_s) \rightarrow Xp_d(n_s)$$

(subscripts s-spectator, d-detected).

The recoil proton can occur with a momentum in the deuteron region due to the effect of Fermi motion of the target nucleons. The transverse component of this momentum enables spectator protons to leave the ISR vacuum chamber and to be detected in the spectrometer. The absence of any deuteron identification in the spectrometer makes it essential to estimate the contamination of break up protons with $x > .85$. In the frame work of the spectator model the shape of the scattered proton spectrum was calculated, via the Monte Carlo method for the two different channels:

$$pp(n_s) \rightarrow pp_d(n_s) \quad (1)$$

$$pn(p_s) \rightarrow p_{s,d}X \quad (2)$$

The Fermi momentum distribution in the deuteron was obtained from the Hamada-Johnston³⁾ wave function in the parametrization of Mc Gee⁴⁾. In both cases the detected proton was restricted to be produced within the angular range of the spectrometer. Fig. 5a) shows the momentum spectrum calculated for process (1); it is compared with the data for elastic events with spectrometer momentum less than 23 GeV/c. The criterion for an elastic event is that only one particle is detected (apart from the spectrometer particle), and is the near collinear direction. The two spectra are normalised to one another at ~ 14.5 GeV/c and show good agreement on the high side of the peak. The slight discrepancy on the low momentum side is due to the falling acceptance, which has not been taken out of the data.

The spectra from process (2) can also be compared and this is shown in Fig. 5b). Again the spectra are normalised to one another at ~ 14.5 GeV/c and again good agreement exists on the high side of the peak. For both cases one finds that above 23 GeV/c, corresponding to a deuteron $x = 0.85$, there is a negligible amount of proton contamination. There is of course the possibility that the spectator proton momentum distribution is distorted by final state interactions, leading to an exaggerated Fermi momentum tail. Evidence against this possibility was obtained from the second spectrometer situated in Intersection 2. Data were taken using this spectrometer during a period when deuterons were circulating in both ISR beams. The reaction

$$dd \rightarrow cX$$

(where c represents a positively charged particle) was studied at a mean production angle of 40 mrad. The ethylene Cerenkov was set to a

pressure of 5 atmospheres, so that protons and deuterons could be distinguished by pulse height measurements above 10 GeV/c. The momentum spectrum of protons and deuterons identified in this way is shown in Fig.6. The contamination of protons above 22 GeV/c is seen to be negligible.

Fig. 7 shows the differential elastic cross-section versus t , as measured in this experiment, for deuteron-proton and proton-proton scattering. In Fig. 8 we present the invariant inelastic differential cross-section for the reaction $dp \rightarrow dX$ versus the mass squared of X at three fixed values of t . For comparison we also plot the spectrum versus M_X^2 at the same values of t for the reaction $pp \rightarrow pX$ scaled down by the measured ratio of the differential elastic cross-sections for the two reactions. All errors are purely statistical. Analysis is still in progress especially concerning systematic errors. But even though the absolute normalisation may be incorrect the internal relative normalisation is believed to be very good.

The striking feature of this graph is the resemblance between the proton-proton and proton-deuteron spectra over the whole M_X^2 range. This is not a priori expected, as discussed above. It thus casts some doubts on the Triple Regge analysis which has been performed so far and may indicate that also the assumed non-diffractive background in high x p-p interactions is dominated by Isospin zero exchanges.

References

1. A.H. Mueller, Phys. Rev. D2 2963 (1970).
2. T. Inami, R.G. Roberts, RL-75-025.
3. T. Hamada, I.D. Johnston, Nucl. Phys. 34 (1962) 382.
4. I.J. McGee, Phys. Rev. 151 (1966) 772.
5. M.G. Albrow et al., Phys. Letters 42B (1972) 279.

Figure captions

- Fig. 1 Schematic drawing of the magnetic spectrometer and scintillation counter hodoscopes.
- Fig. 2a) Diagram of the quasi-two-body process $ab \rightarrow cX$.
2b) The associated Triple Regge diagram.
- Fig. 3 Fit to inelastic proton spectrum at $s = 551$ and $t = - .15$ performed by T. Inami and R.G. Roberts.
- Fig. 4 Observed momentum spectrum integrated over the angular range of the spectrometer not corrected for momentum acceptance.
- Fig. 5a) Calculated momentum distribution for the reaction $pp(n_s) \rightarrow pp_d(n_s)$ compared with elastic data. The two spectra are normalised so as to coincide 14,5 GeV/c.
5b) Comparison between calculated spectrum for the reaction $pn(p_s) \rightarrow (p_{s,d})X$ and data. (Again normalised at 14,5 GeV/c).
- Fig. 6 Spectrum obtained from the reaction $dd \rightarrow cX$. The positively charged particle c was identified as indicated, using pulse height information from an ethylene Cerenkov counter.
- Fig. 7 Differential elastic cross-section versus t for the reactions
● : $dp \rightarrow dp$
○ : $pp \rightarrow pp$.
- Fig. 8 Inelastic invariant differential cross-section versus M_x^2 at
a) $t = - .22 \text{ (GeV/c)}^2$
b) $t = - .26 \text{ (GeV/c)}^2$
c) $t = - .30 \text{ (GeV/c)}^2$.
● $pp \rightarrow pX$
○ $pd \rightarrow dX$

1. The first part of the document discusses the importance of maintaining accurate records of all transactions and activities. It emphasizes the need for transparency and accountability in financial reporting.

2. The second part of the document outlines the various methods and techniques used to collect and analyze data. It includes a detailed description of the experimental procedures and the statistical tools employed.

3. The third part of the document presents the results of the study, including a comparison of the different methods and a discussion of the implications of the findings. It also includes a table of the data collected during the experiment.

4. The fourth part of the document discusses the limitations of the study and suggests areas for future research. It also includes a conclusion that summarizes the main findings and the overall significance of the work.

5. The fifth part of the document provides a detailed description of the experimental setup and the equipment used. It includes a list of the materials and reagents used, as well as a description of the safety protocols followed during the experiment.

6. The sixth part of the document discusses the ethical considerations of the study and the steps taken to ensure the safety and well-being of the participants. It also includes a statement of the author's commitment to the highest standards of research integrity.

7. The seventh part of the document provides a detailed description of the data analysis process, including the software used and the specific statistical tests applied. It also includes a discussion of the potential sources of error and the steps taken to minimize their impact.

8. The eighth part of the document discusses the broader context of the study and its relevance to the field of research. It includes a comparison of the findings with those of other studies and a discussion of the potential applications of the results.

9. The ninth part of the document provides a detailed description of the experimental results, including a comparison of the different methods and a discussion of the implications of the findings. It also includes a table of the data collected during the experiment.

10. The tenth part of the document discusses the limitations of the study and suggests areas for future research. It also includes a conclusion that summarizes the main findings and the overall significance of the work.

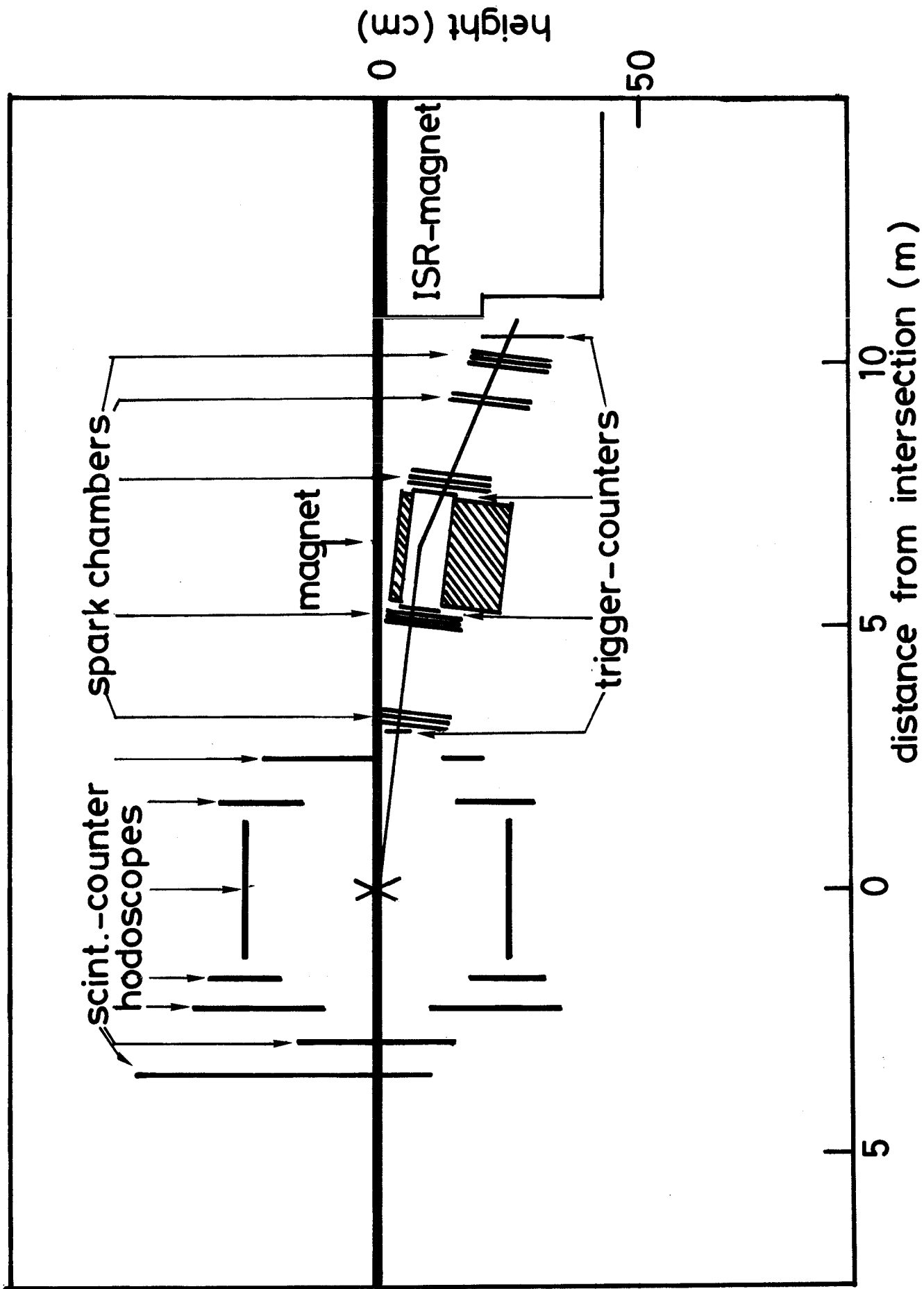


Fig.1

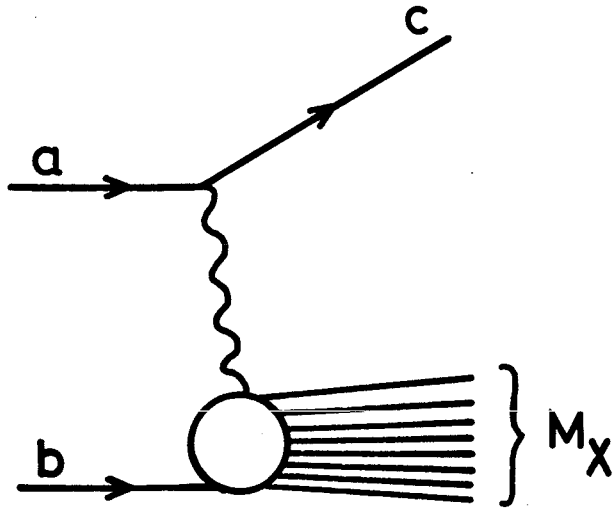


Fig.2a)

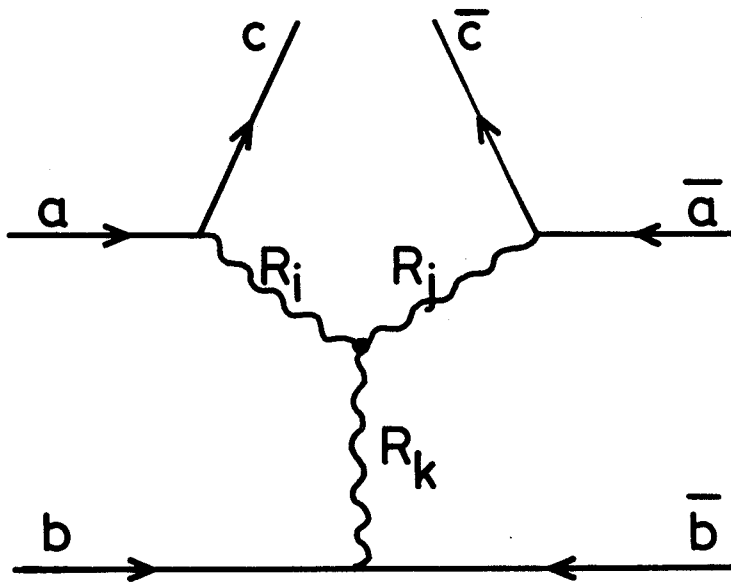


Fig.2b)

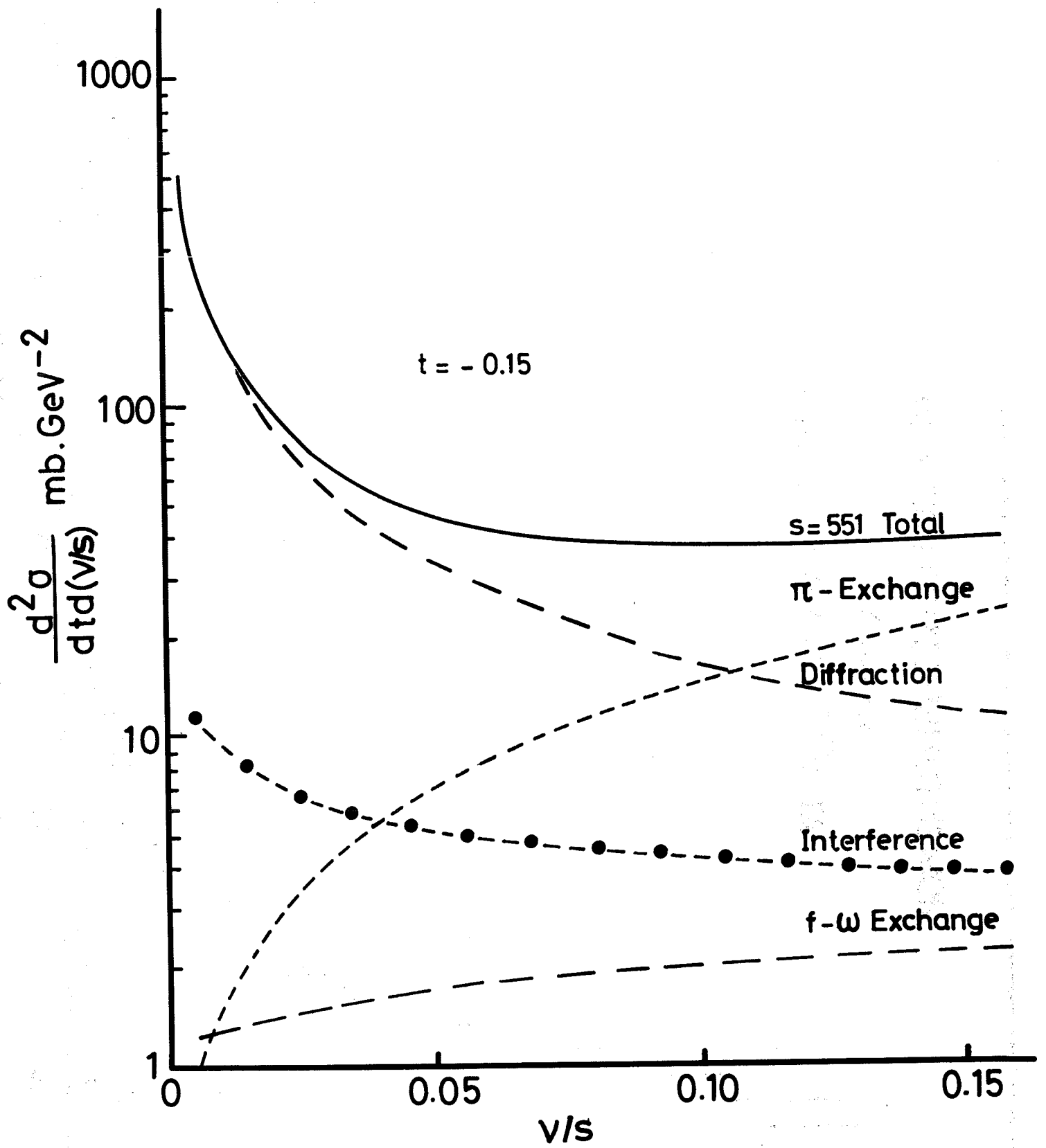


Fig.3

MOMENTUMSPECTRUM OF c IN

pd → cX

AT $\sqrt{S} = 52.8$ GeV ; 18 mrad.

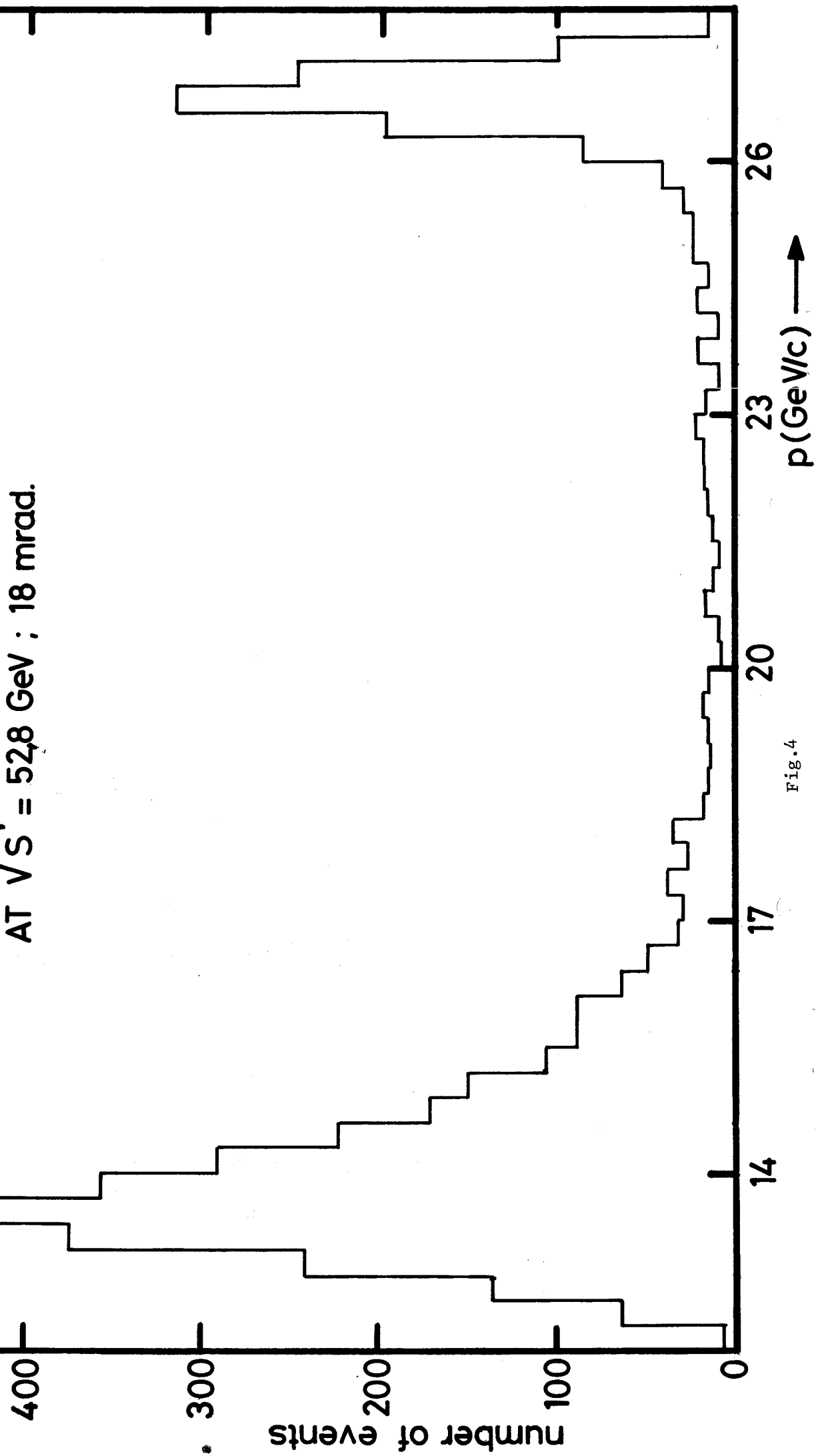
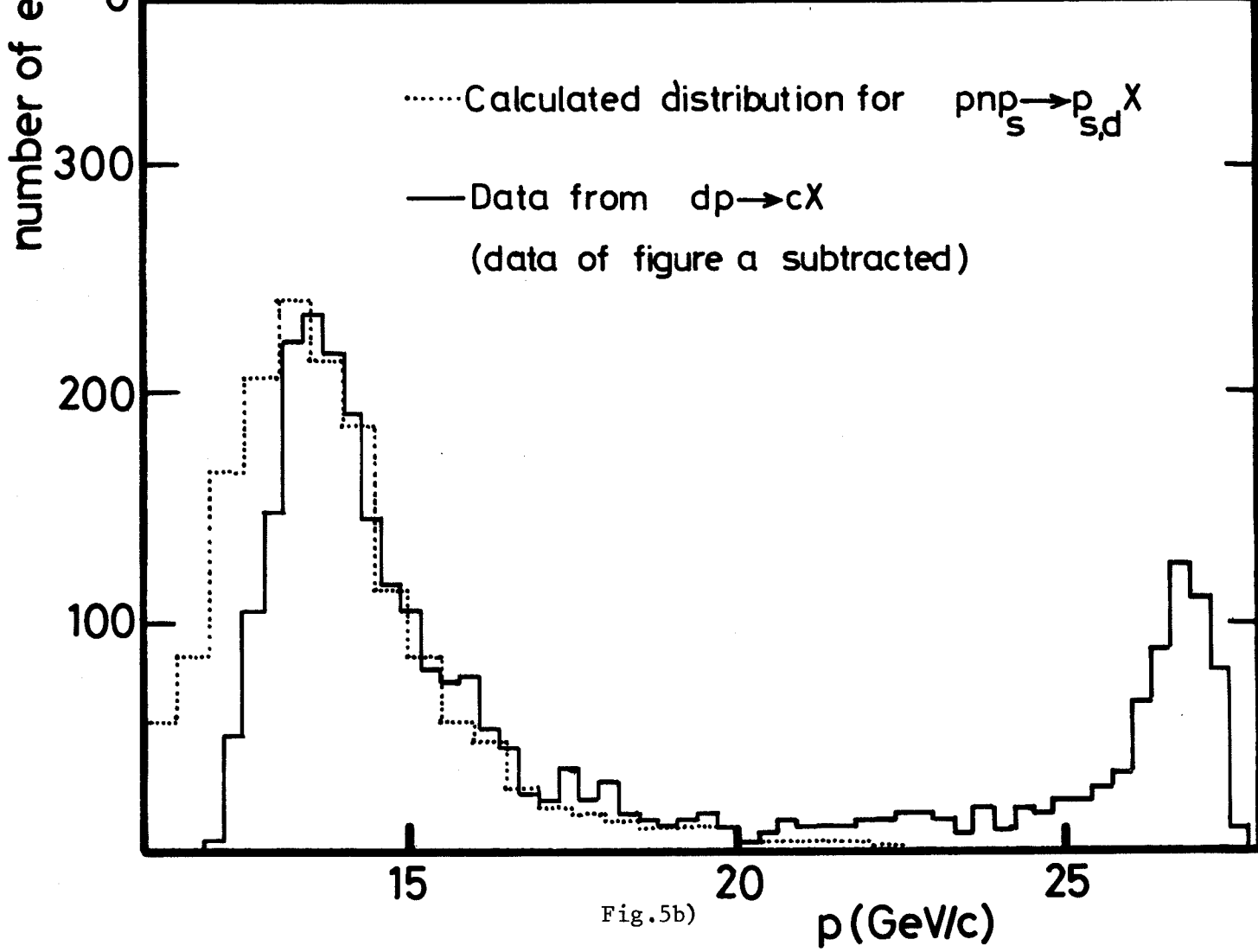
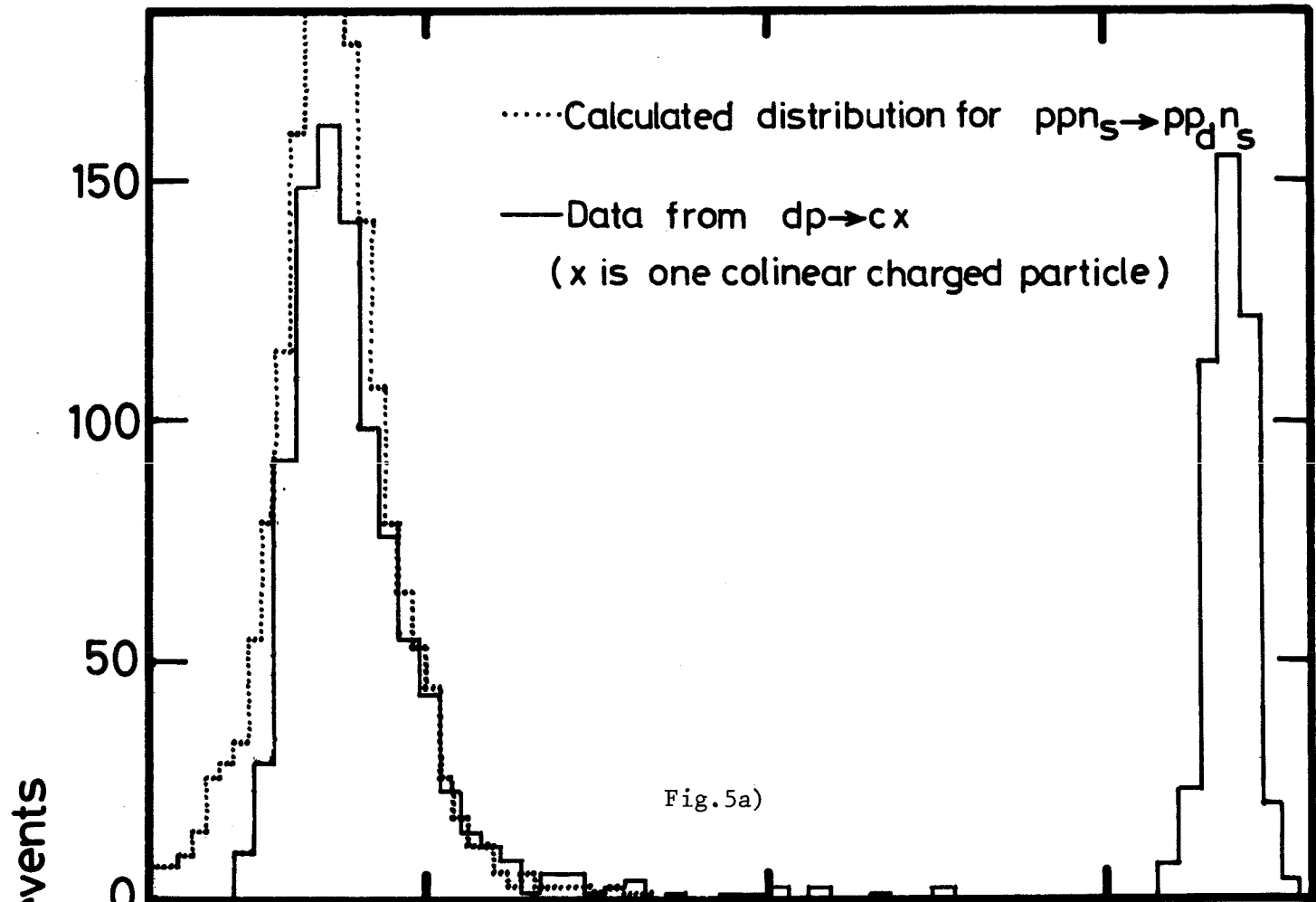


Fig.4



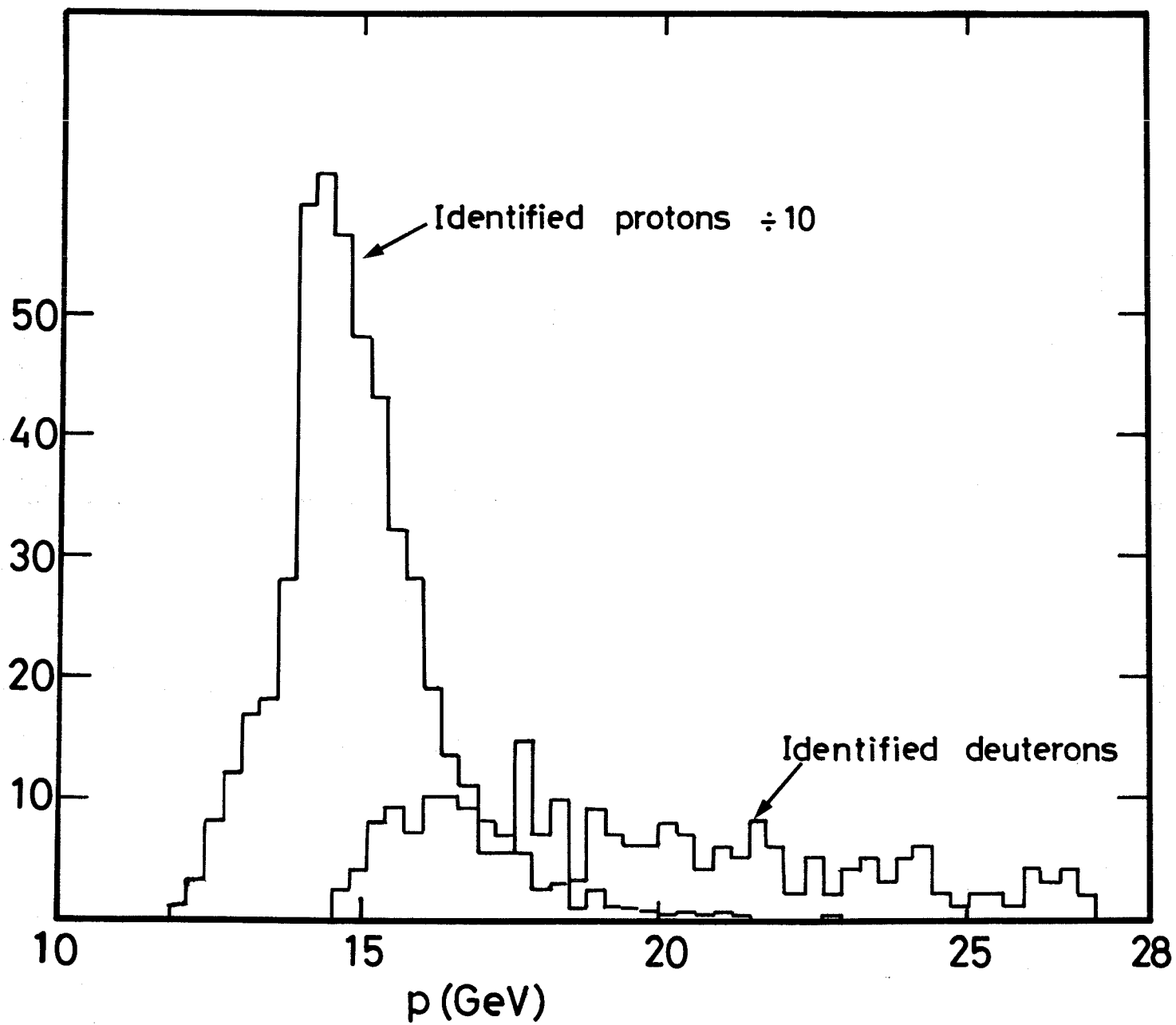


Fig.6

ELASTIC DIFFERENTIAL CROSS-SECTION
VERSUS T AT S=2780 GeV²

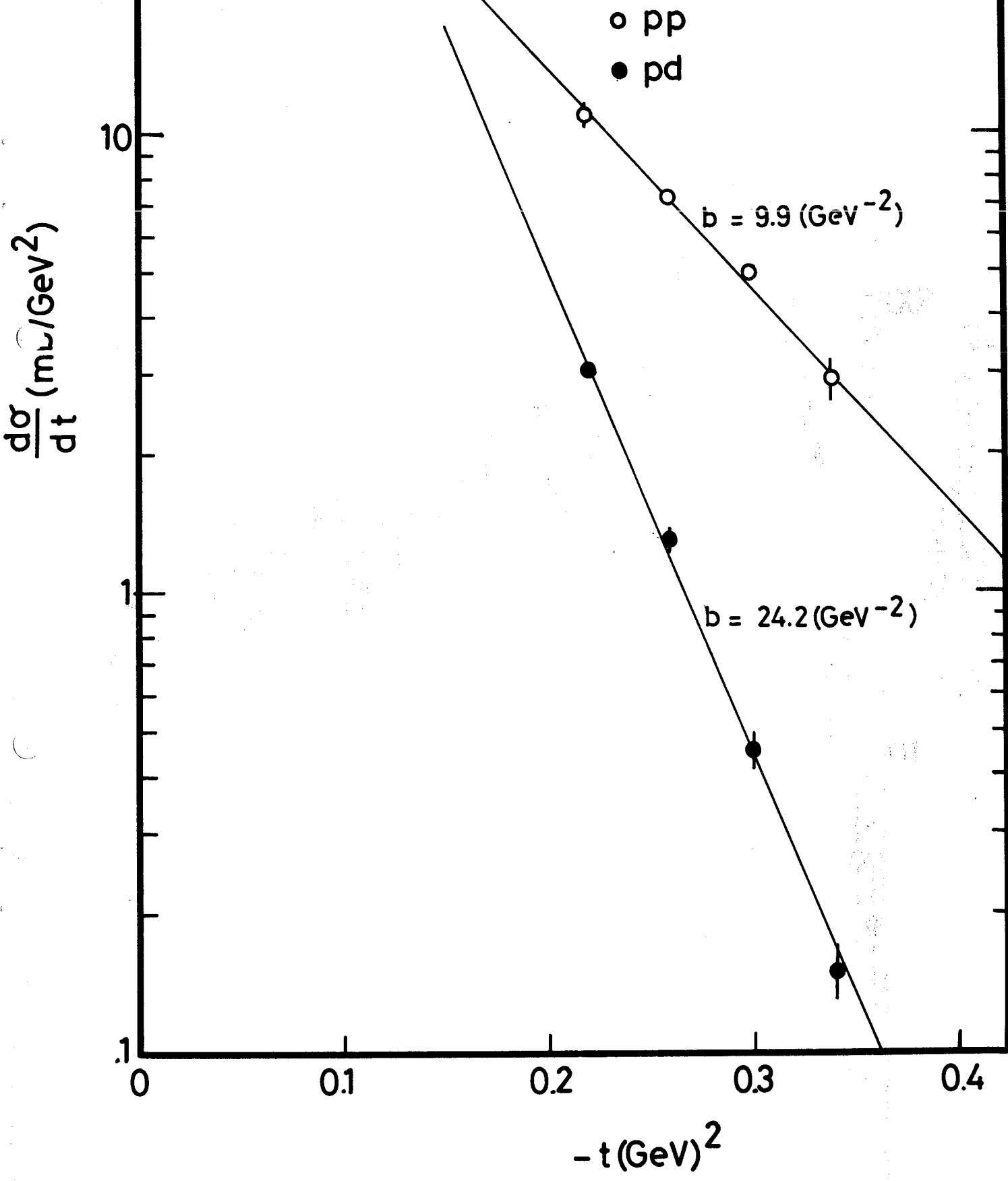


Fig.7

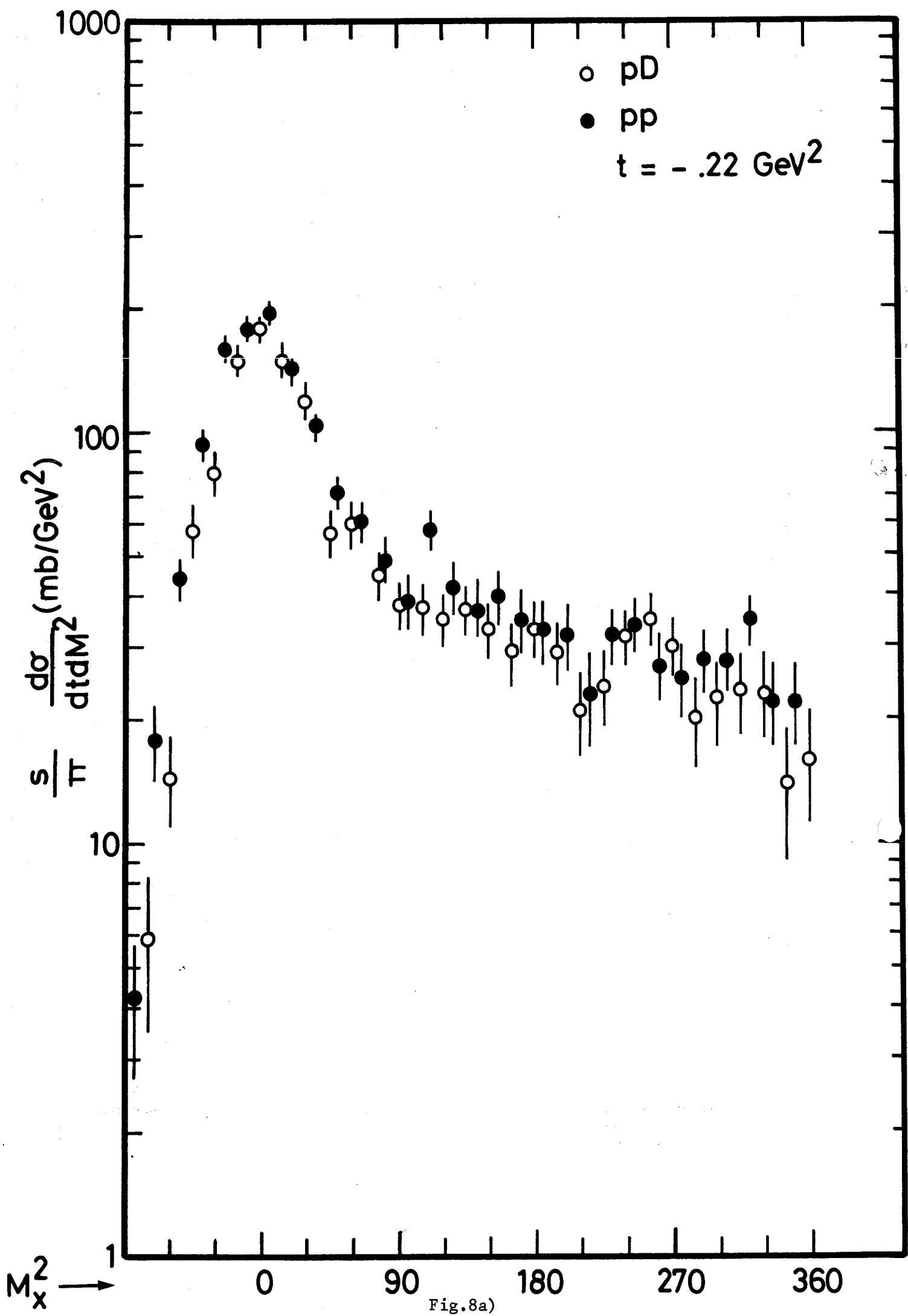


Fig. 8a)

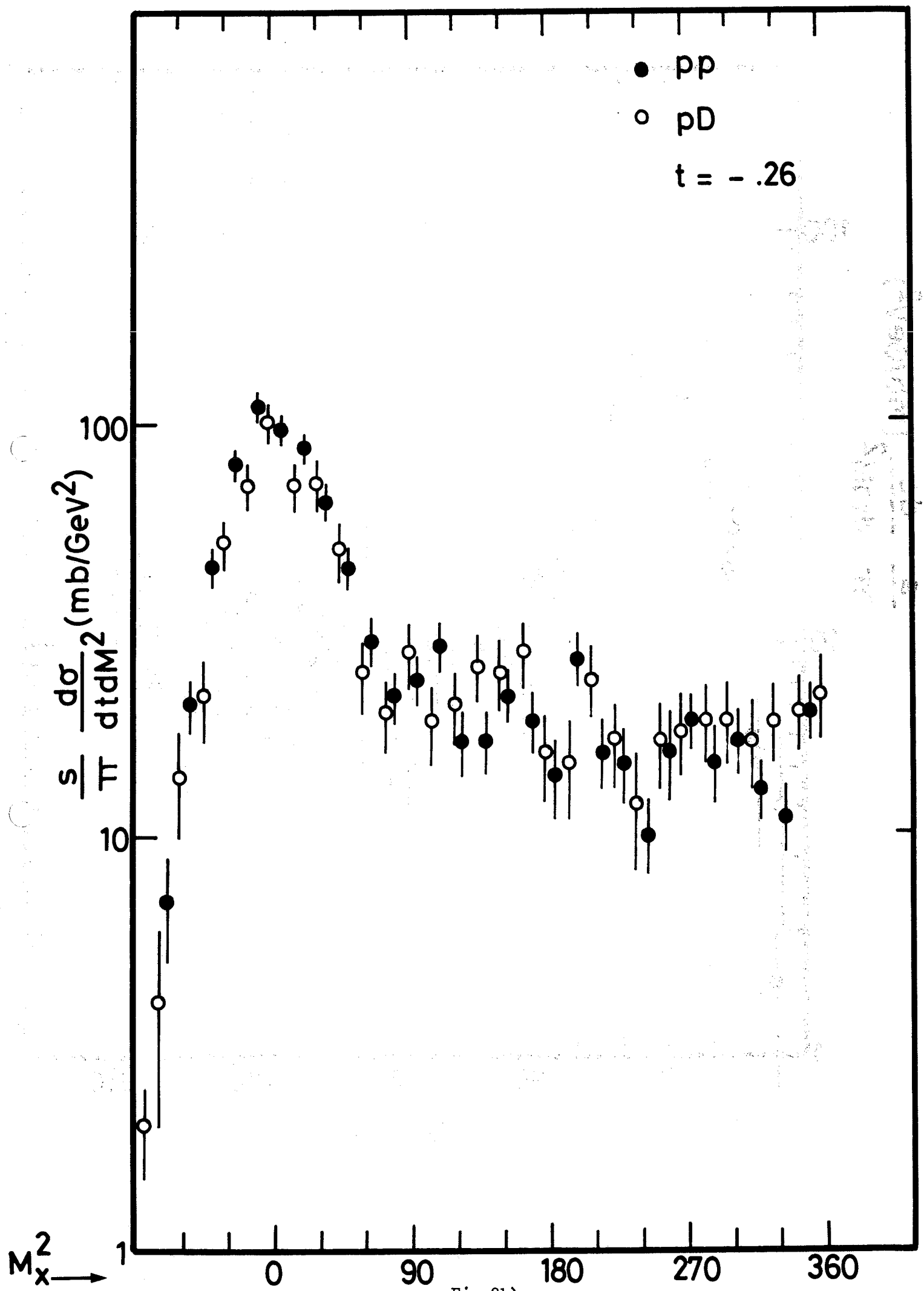


Fig.8b)

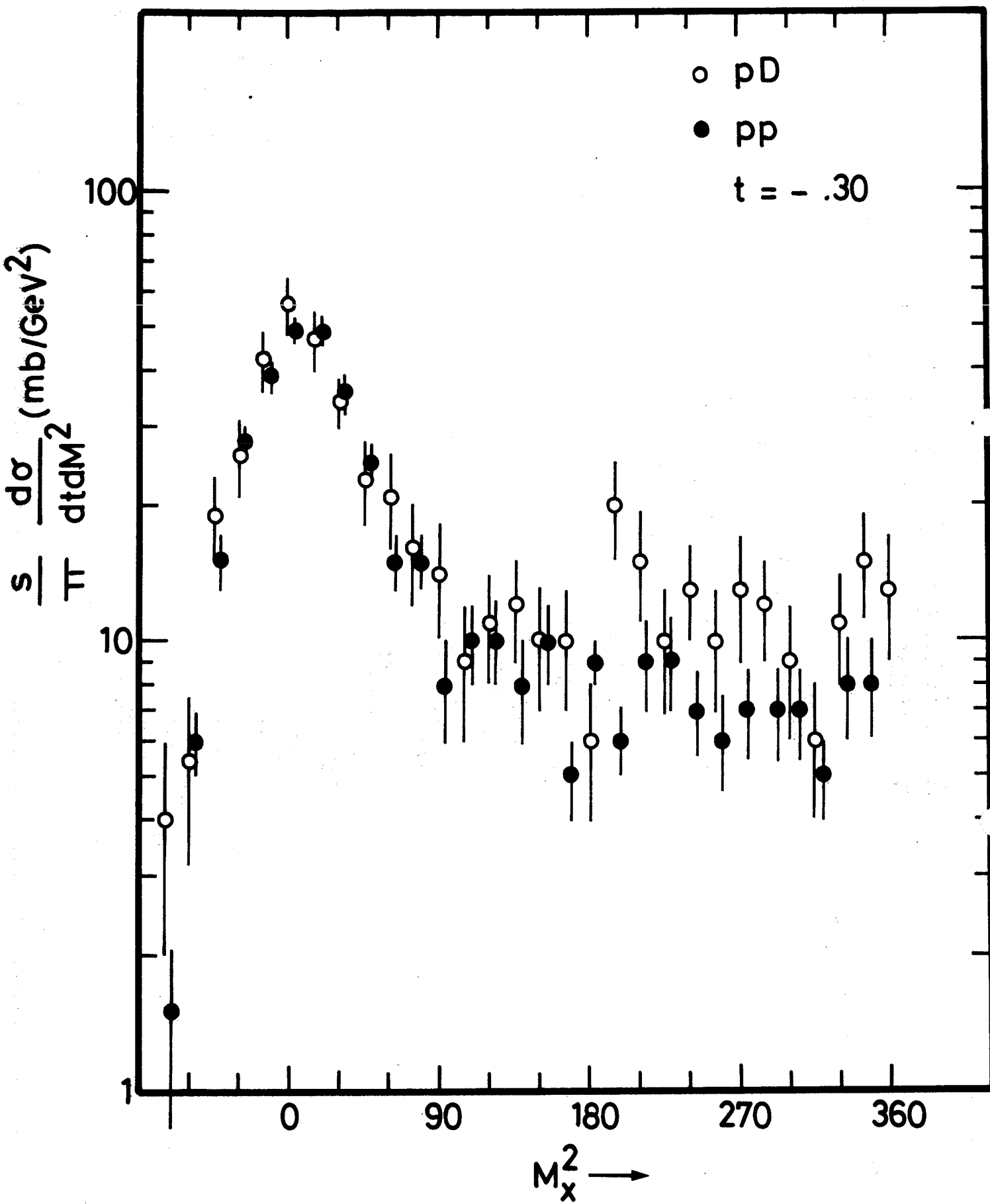


Fig.8c)